IEEE Access
Multidisciplinary | Rapid Review | Open Access Journal

Received October 22, 2018, accepted November 18, 2018, date of publication December 10, 2018,
date of current version December 31, 2018.

Digital Object Identifier 10.1109/ACCESS.2018.2883677

Wind Speed Extrapolation Using Machine Learning Methods and LiDAR Measurements

M. A. MOHANDES AND S. REHMAN
King Fahd University of Petroleum & Minerals, Dhahran 31261, Saudi Arabia

Corresponding author: M. A. Mohandes (mohandes@kfupm.edu.sa)

This work was supported by the National Plan for Science, Technology, and Innovation (MAARIFAH), King Abdulaziz City for Science and Technology, through the Science and Technology Unit at the King Fahd University of Petroleum & Minerals (KFUPM) under Grant 12-ENE2384-04.

ABSTRACT Accurate wind energy assessments require wind speed (WS) at the hub height. The cost of WS measurements grows enormously with height. This paper utilizes deep neural network (DNN) algorithm for the extrapolation of the WS to higher heights based on measured values at lower heights. LiDAR measurements at lower heights are used for training the system and at higher heights for performance analysis. These measurements are made at 10, 20, . . . , and 120 m heights. First, the measured WS values at 10–40 m were used to extrapolate values up to 120 m. In the second scenario, the WS at 10–50 m were used to extrapolate values up to 120 m. This continued until the last scenario, in which the WS at 10–100 m were used to estimate values at 110 and 120 m. A relationship between heights of measurements and the accuracy of the WS estimation at hub height is presented. The WS extrapolated using the present approach is compared with the measured values and with local wind shear exponent (LWSE)-based extrapolated WS. Furthermore, to analyze the performance of the DNN relative to other machine learning methods, we compared its performance with that of classical feedforward artificial neural networks trained using a genetic algorithm to find the initial weights and the Levemberg–Marquardt (LM) method (GANN) for training. The mean absolute percent error between measured and extrapolated WS at height 120 m based on measurements between 10–50 m using DNN, GANN, and LWSE are 9.65%, 12.77%, and 9.79%, respectively.

INDEX TERMS Extrapolation, machine learning, renewable energy, wind speed profile.

I. INTRODUCTION

Generally, the energy output of a wind turbine increases with increasing wind speed (WS). However, the WS at a site increases with height due to less gravitational pull and the leaning up of frictional forces at higher heights. Hence there is a need to conduct WS measurements at higher heights either using wind masts or LiDAR type of equipment for accurate wind energy resource assessment. Both of these approaches are costly and skilled manpower intensive [1]. On the cost front of wind speed measurements, a 60m tall tower costs around US $45,000 while an 80-meter lattice tower costs more than US $85,000 [2]. Commonly, the hub heights of modern wind turbines range from 60 to 120m for on-shore applications and more for offshore installations. Therefore, it motivates to develop models and methodologies which can provide better estimates of WS at hub height using the available measured WS at lower heights. Hence accurate wind measurements are required up to the wind turbine hub height for risk free investment.

The behavior of vertical wind speed profile over homogeneous land in stationary conditions can be estimated accurately within the first 30 to 60m above ground level using Monin-Obukhov Similarity Theory (MOST) and surface-layer scaling [3]–[7]. Beyond these levels the vertical WS profile progressively deviates from MOST due to the influence of other parameters such as the boundary-layer height [7], [8]. However, it has been observed that marine wind speed profile does not follow the MOST profile starting at heights as low as 29m above mean sea level (AMSL) [9]. Lange *et al.* [10] and Peña and Gryning [11] found deviations in near-neutral and stable conditions at 45-50m AMSL. Gualtieri [12] extrapolated WS to 100m using α–I method in conjunction with turbulence intensity measurements at 30m with a bias of less than 5%, RMSE $= 0.20$, and $R^2 = 0.94$. In another study, Gualtieri and Secci [13] analyzed the performance of several theoretical methods for WS profile estimation and indicated that their accuracies depend highly on the atmospheric stability conditions.

Empirical methods rely mainly on the logarithmic and power law calculations. However, Newman and Klein [14] found that the power law performed well under neutrally stable atmospheric situations and failed under unstable conditions and hence has limitations. Local wind shear exponent (LWSE) model is based on the empirical value of the shear exponent which is calculated using the local wind speed measurements made at different heights at the site of interest. It provides good extrapolated wind speed compared to the above theoretical methods. However, it is highly site dependent and relies on class one quality wind anemometer based measurements. Ayodele *et al*. [15] used measured wind speeds at 20 and 60m to estimate the LWSE and then carried out wind power assessment with better accuracy. Tizpar *et al*. [16] used wind speed measurements at 10, 30, and 40m to estimate the LWSE and then obtained reliable wind power potential assessment at hub height. In Northern Cyprus, Solyali *et al*. [17] calculated the LWSE using wind measurements at 50, 80, and 90m and then extrapolated the wind speed to the required hub height for accurate wind power potential.

Hence to overcome the complexity and the cost burden related to the above approaches, which most countries cannot afford, modelling approaches are being used to extrapolate the WSs to required hub heights using historically available data. The present study aims at using Deep Neural Networks (DNN) to estimate the WS at the hub height based on measurements at lower heights. A large number of artificial neural networks methodologies have been used for temporal and spatial wind speed estimations [18]–[23]. Limited work has been reported in the literature on the use of machine learning methods for vertical wind speed estimation [24]–[26]. Turkan *et al*. [25] compared the performance of seven different machine learning methods to estimate WS at 30m heights based on measurements at 10m height. Saiful Islam *et al*. [26] used wind speed data measured at 10-40m at Juaymah meteorological station in Saudi Arabia and extrapolated the WS up to 100m height. Authors used two hybrid neural networks, namely, Genetic algorithm and particle swarm optimization. They had no measured data except up to 40m, therefore, they compared their extrapolation results with 1/7 power law and logarithmic law.

The contributions of this paper can be summarized as follows:

- It represents the first use of deep neural networks for vertical WS extrapolation.
- It shows users the measurements needed at lower heights to achieve a specified amount error at the hub height.
- It shows that DNN outperforms other machine learning method (GANN) and a classical non-machine learning method (LWSE)
- It compares extrapolated WS values with real measured values up to height of 120m.

The paper is organized as follows: Section II describes the methodology used. Section III discusses the experimental results, while analysis of performance is provided in Section IV. Finally conclusions and future works are summarized in Section V.

FIGURE 1. ZephIR 300 Onshore Wind Lidar.

II. METHODOLOGY USED

Laser Doppler (LiDAR) anemometry devices have gained significant maturity in recent years, both in terms of reliability and measurement quality. These techniques are being increasingly applied in routine wind measurement campaigns as can be seen from the studies reported in the literature [27]–[31]. The LiDAR anemometers have many advantages, including ease and low cost of installation and decommissioning, measurements to blade tip and above, re-usability, no calibration drift, no permits requirement, no aviation obstruction, no mast or boom flow distortions, no icing affects, and reduced lightning vulnerability.

The acquired LiDAR (shown in Fig. 1) was deployed at a secured site in Dhahran (inside the campus of King Fahd University of Petroleum and Minerals). The unit can measure WS up to 200m height in the range of 2-50m/s within -5 to 50°C ambient temperatures. Dhahran is an on-shore site 15 km away from the Gulf coast with a flat terrain. There are some short trees around the site which experiences normal diurnal changes of temperature and wind speed.

Deep Neural Networks (DNN) is finding wide real life applications lately. A DNN is a feed-forward Artificial Neural Network (ANN) with more than one hidden layer between its inputs and the outputs. DNN has shown its significant superiority over shallow ANN on modelling data for speech recognition, image recognition, classification, and dimensionality reduction [32], [33]. DNN with multiple hidden layers and large number of units per layer can model extremely complex and non-linear relationships between inputs and outputs from training data.

Rehman [33] proposed a generative pre-training to model the structure of the available data. After pre-training, near optimal initial weights are obtained and fine-tuning is performed using regular backpropagation learning. In addition to providing near optimal initial weights, the Restricted Boltzmann Machine (RBM) pre-training also enhances generalization since most of the information in the weights is drawn from sampling the data [33]. Pre-training is performed by

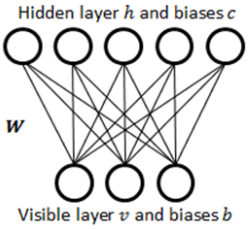

FIGURE 2. RBM architecture.

decomposing each layer as an input-output pair. Each pair is then treated as a RBM which consists of two layers namely visible (v) and hidden (h) (Fig. 2). The biases b and c denote the visible and hidden layer biases. The visible and hidden units are connected with weights W. The initial values of the weights and biases are assumed random with Gaussian distribution N(0, 0.1).

For each iteration, the pre-training takes two phases i.e. a positive and a negative. First, in the positive phase, we set the training vector x as the values of the visible units (v^+). The value of each hidden unit (h_j^+) is set to one with probability

$$\hat{h}_j^+ = p\left(h_j^+ = 1|v^+\right) = \sigma\left(c_j + \sum_i v_i^+ w_{ij}\right) \quad (1)$$

where $\sigma(x)$ is the logistic sigmoid function $1/(1+\exp(-x))$. The values from the positive phase h_j^+ are used to calculate the values in the negative phase as follows:

$$\hat{v}_i^- = \sigma\left(b_i + \sum_j h_j^+ w_{ij}\right) \quad (2)$$

$$\hat{h}_j^- = \sigma\left(c_j + \sum_i \hat{v}_i^- w_{ij}\right). \quad (3)$$

Finally, the updates for the weights and biases are given by:

$$\Delta w_{ij} = \epsilon\left(\langle v_i \hat{h}_j\rangle^+ - \langle \hat{v}_i \hat{h}_j\rangle^-\right) \quad (4)$$

$$\Delta b_i = \epsilon\left(\langle v_i\rangle^+ - \langle \hat{v}_i\rangle^-\right) \quad (5)$$

$$\Delta c_j = \epsilon\left(\langle \hat{h}_j\rangle^+ - \langle \hat{h}_j\rangle^-\right) \quad (6)$$

where $\langle\cdot\rangle$ denotes expectation operator over all data and ϵ is the learning rate. Superscripts $+$ and $-$ indicate the positive and negative phases, respectively. This process is repeated for a pre-set maximum number of iterations. The same procedure is applied for the next RBM using the outputs of the previous RBM as inputs to the current one. This process continues until the last RBM. The weights and biases obtained from this pre-training process are used as initial values for a feedforward network obtained by stacking the RBM pairs in sequence. This resultant network is trained using regular feedforward backpropagation for fine tuning. The training process continues until the error between the desired output and the real output layer reaches a pre-determined value or a maximum number of iterations.

In our experiments, we divided the measurement data into training part (50%), cross validation part (25%) and testing part (25%). Based on the performance of cross validation data, 50 iterations are used for pre-training of each RBM with a unified learning rate of 0.1 for all weights and biases. Five RBMs were pre-trained to generate initial weights and biases for four hidden layers with 30-20-15-10 units. All units used sigmoid activation units. The fine-tuning was done using the regular back-propagation technique with a learning rate of 0.001 and a maximum number of iterations of 1000.

For performance evaluation, several measures are used including mean absolute percent error (MAPE), root mean square error (RMSE), and mean biased error (MBE). These error parameters are calculated using the following equations [34]:

$$MAPE = \frac{1}{N}\sum_{i=1}^{N}\left|\frac{M_i - E_i}{M_i}\right| \quad (7)$$

$$RMSE = \sqrt{\frac{1}{N}\sum_{i=1}^{N}(M_i - E_i)^2} \quad (8)$$

$$MBE = \frac{\sum_{i=1}^{N}(M_i - E_i)}{N} \quad (9)$$

where N is the number of samples, M and E are the measured and the estimated values of the WS.

III. EXPERIMENTAL RESULTS

In practice wind measurements are mostly available up to 40 meters. In such cases the WS is extrapolated to the required hub height using the 1/7th power law or LWSE. Usually, such extrapolations deviate significantly from real values. In this study, WS data was collected by the LiDAR system between June 15, 2015 and July 4, 2016. The WS data was scanned every second and was stored as 10-minute averages. Hourly averaged WS values were calculated at heights 10-120m. The DNN technique described above was used to estimate WS at higher heights. Several cases have been considered. In the first scenario, WS at 10-40m were used to estimate values at heights 50-120m. In the second scenario, values at 10-50m were used to estimate WS at 60-120m. Scenarios continued in the same way until the last scenario where WS at 10-100m were used to estimate values at 110 and 120m. The results of the extrapolation process for all scenarios are given in tables. Detailed results are given in figures for two scenarios only: one using measurements at 10-50m and the other using measurements at 10-80m, as representatives of the performance of the proposed methods.

The extrapolation process in the first scenario was accomplished by training a DNN system on WS values at 10, 20, and 30m as inputs and WS at 40m as the output. The same trained system was provided with WS values at 20, 30, and 40m as inputs to estimate WS at 50m. Hence, the system extrapolates WS from three lower measurements to one step higher. In the next step, the measured WS at 10-40m along with the newly estimated value at 50m were used to train a new DNN system with 4 inputs and one output. This trained system was provided with WS values at 20-50m to extrapolate to the next height at 60m. This process of using measured and estimated WS values at lower heights to find WS values at one step higher height continued until we obtained WS at 120m.

TABLE 1. Assessment of estimated WS at heights 50-120m based on measurements at 10-40M.

Method	Deep neural network								Local wind shear exponent							
Height (m)	50	60	70	80	90	100	110	120	50	60	70	80	90	100	110	120
MAPE (%)	2.06	4.19	5.63	7.15	8.4	9.65	10.65	11.66	3.02	5.33	7.58	9.58	11.41	13.09	14.60	15.99
RMSE	0.03	0.1	0.2	0.37	0.55	0.78	1	1.25	0.04	0.13	0.30	0.52	0.80	1.13	1.50	1.92
MBE	0.05	0.16	0.21	0.28	0.31	0.35	0.36	0.38	-0.07	-0.09	-0.17	-0.23	-0.30	-0.35	-0.43	-0.49
R^2 (%)	99.6	98.27	96.73	94.44	92.23	89.5	87.29	84.73	99.27	97.78	95.63	93.16	90.43	87.56	81.78	81.80

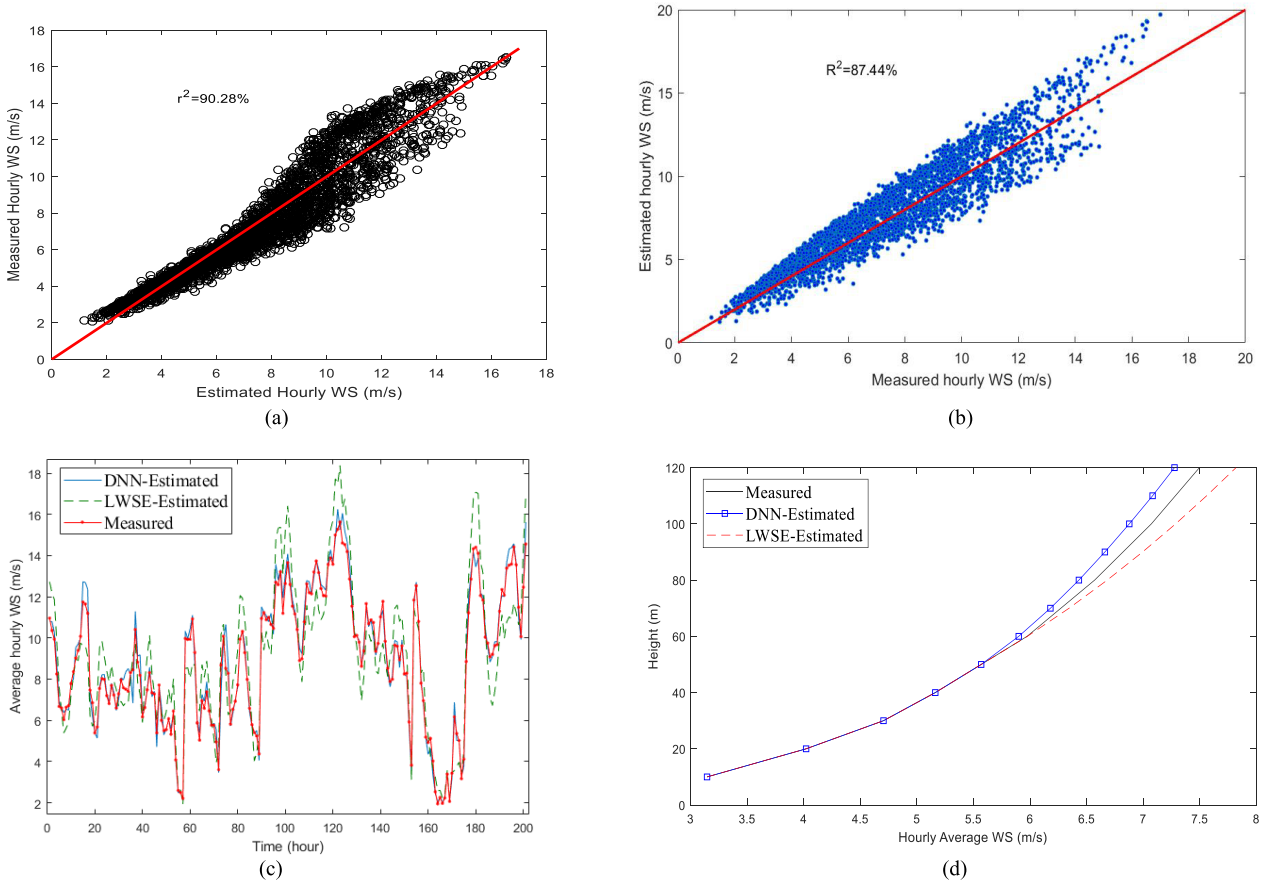

FIGURE 3. Results for estimation of WS at 120m based on measurements between 10-50m (a) The scatter plot of measured and estimated wind speed at 120m using DNN, (b) The scatter plot of measured and estimated wind speed at 120m using LWSE, (c). Estimated and measured hourly WS at a sample range, (d). Average vertical profiles of measured and estimated wind speed values.

Using the same measured WS at 10-40m we extrapolated to higher heights (50-120m) using LWSE method.

Table 1 shows the error values MAPE, RMSE, and MBE between the measured and estimated WS values at heights between 50 and 120m for both DNN and LWSE methods. The MAPE varied between 2.06% at 50m to 11.66% at 120m, corresponding to the proposed method while between 3.02% and 15.99% corresponding to LWSE based estimations. Similarly, the RMSE values varied from 0.03 to 1.25m/s and 0.04 to 1.92m/s corresponding to DNN and LWSE methods, respectively. These values indicate that the error increases with the addition of estimated WSs with measurements between 10-40m in both the methods. However, the MBE values showed a positive bias for DNN method (overestimation) and a negative bias (underestimation) for LWSE approach. The coefficient of determination R^2 values are found to be higher in case of DNN method compared to that LWSE based estimations an indication of superior performance.

For the second scenario, measured WS at 10-50m were used to estimate values at 60-120m following the same procedure as in the first scenario. Fig. 3(a) shows the scatter plot of the measured and estimated WSs at 120m using DNN method with R^2 value of 90.28%, while Fig 3(b) shows the scatter plot for LWSE method with R^2 value of 87.44%. The plot shows a small scatter for lower WS up to 5m/s and then the scatter increases for higher WS values. The estimated and measured values at 120m are compared in Fig. 3(c) for

TABLE 2. Assessment of estimated WS at heights 60-120m based on measurements at 10-50M.

Method	Deep neural network							Local wind shear exponent						
Height (m)	60	70	80	90	100	110	120	60	70	80	90	100	110	120
MAPE (%)	1.33	2.38	3.93	5.4	6.95	8.27	9.65	2.32	4.48	6.46	8.26	9.92	11.39	12.77
RMSE	0.02	0.05	0.14	0.27	0.46	0.68	0.97	0.03	0.10	0.24	0.42	0.66	0.93	1.24
MBE	0.08	0.1	0.14	0.15	0.17	0.15	0.13	-0.00	-0.07	-0.11	-0.17	-0.21	-0.28	-0.32
R^2 *(%)*	99.76	99.2	97.98	96.42	94.37	92.48	90.28	99.55	98.40	96.69	94.64	92.31	89.96	87.44

TABLE 3. Assessment of estimated WS at heights 70-120m based on measurements at 10-60M.

Method	Deep neural network						Local wind shear exponent					
Height (m)	70	80	90	100	110	120	70	80	90	100	110	120
MAPE (%)	0.99	1.97	3.18	4.36	5.71	7.07	2.33	4.31	6.14	7.81	9.28	10.66
RMSE	0.01	0.03	0.08	0.16	0.28	0.45	0.03	0.29	0.24	0.42	0.63	0.88
MBE	0.01	-0.01	-0.04	-0.02	-0.08	-0.11	-0.06	-0.09	-0.14	-0.18	-0.23	-0.27
R^2 *(%)*	99.9	99.57	98.95	98.04	96.79	95.19	99.54	98.44	96.87	94.98	92.96	90.75

TABLE 4. Assessment of estimated WS at heights 80-120m based on measurements at 10-70M.

Method	Deep neural network					Local wind shear exponent				
Height (m)	80	90	100	110	120	80	90	100	110	120
MAPE (%)	1.1	2.02	3.45	4.43	5.69	1.95	3.75	5.40	6.86	8.24
RMSE	0.02	0.04	0.11	0.18	0.3	0.02	0.09	0.20	0.35	0.54
MBE	0	0	-0.03	-0.06	-0.1	-0.02	-0.06	-0.09	-0.13	-0.17
R^2 *(%)*	99.84	99.52	98.69	98.01	96.8	99.67	98.79	97.48	95.97	94.19

TABLE 5. Assessment of estimated WS at heights 90-120m based on measurements at 10-80M.

Method	Deep neural network				Local wind shear exponent			
Height (m)	90	100	110	120	90	100	110	120
MAPE	0.9	1.64	2.66	3.69	1.86	3.51	4.99	6.37
RMSE	0.01	0.03	0.08	0.15	0.02	0.09	0.19	0.33
MBE	0	-0.02	-0.05	-0.1	-0.04	-0.05	-0.09	-0.12
R^2 *(%)*	99.91	99.69	99.18	98.45	99.69	98.88	97.77	96.36

a sample range. In this case, the estimated WSs followed the trend of measured values closer than that in the first scenario. This improvement in the estimated WS values is associated with the addition of one more level of measured WS at 50m. The average vertical profiles of estimated (using LWSE, $1/7^{th}$ power law, and DNN methods) and measured WS values are compared in Fig. 3(d). The figure indicates that WS profile obtained using the DNN method is closer to the measured profile compared to other methods. Performance of the proposed method and the LWSE are shown in Table 2 for all the heights.

In the third scenario, WSs at heights 70-120m were estimated using measurements at 10-60m following the same procedures as in first two scenarios. The error magnitudes between the measured and estimated values of WS for both the methods at different heights are summarized in Table 3. The MAPE values show linearly increasing trends from 0.99% to 7.07% while moving from lower to higher heights in the case of DNN method, outperforming the values for LWSE. The RMSE values were slightly higher in case of LWSE approach compared to DNN method. The estimated WS values using the DNN and LWSE methods were overestimated and underestimated, respectively, as can be observed from positive and negative values of MBE. The coefficient of determination R^2 values are observed to be higher in case of DNN estimations compared to LWSE based estimated values.

In the fourth scenario, WS values were estimated between 80 to 120m using the measured WS at 10-70m in a process similar to the previous three scenarios. The performance measures at 80 to 120m heights between the estimated and measured WS values are provided in Table 4. The error values showed an increasing trend with height but the magnitude of these terms was less than those in the previous cases. In general, lower values of these error terms were observed in cases of DNN estimations compared to LWSE method. The MBE values showed underestimation for both methods. The R^2 values were higher in the case of DNN compared to LWSE, indicating better performance

In the fifth scenario, measured WS values between 10-80m were used to estimate values at 90-120m. The MAPE, RMSE, MBE, and R^2 values are summarized in Table 5, indicating better performance for the proposed method. Outperformance of the proposed method is also indicated in Fig. 4.

In the sixth scenario, measured values between 10 to 90m were used to estimate WS between 100-120m. All performance parameters were found to be better than previous cases

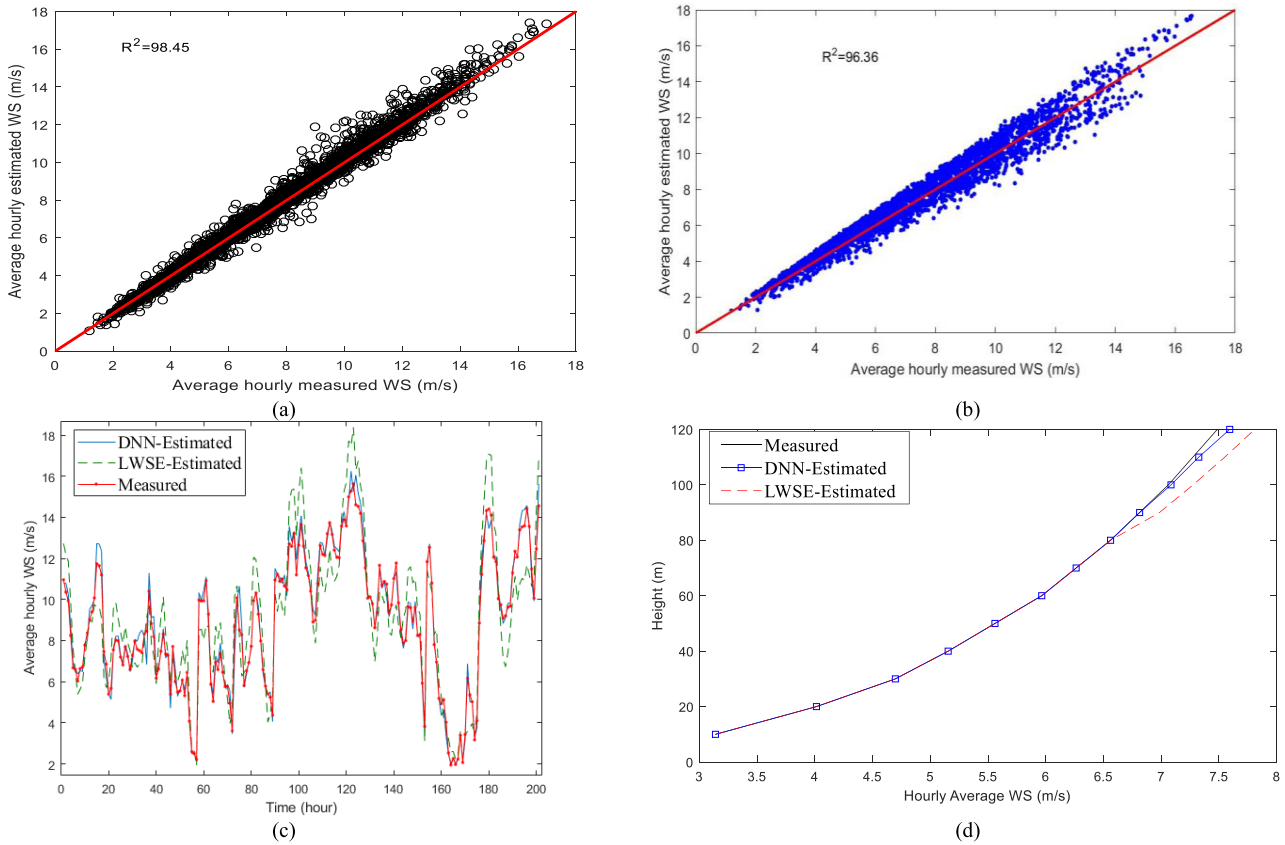

FIGURE 4. Results for estimation of WS at 120m based on measurements between 10-80m, (a) The scatter plot of measured and estimated WS at 120m using DNN, (b) The scatter plot of measured and estimated WS at 120m using LWSE, (c). Estimated and measured hourly WS at a sample range, (d). Average vertical profiles of measured and estimated wind speed values.

TABLE 6. Assessment of estimated WS at heights 100-120m based on measurements at 10-90M.

Method	Deep neural network			Local wind shear exponent		
Height (m)	100	110	120	100	110	120
MAPE	0.63	1.59	2.89	1.64	3.11	4.49
RMSE	0.01	0.03	0.11	0.02	0.07	0.17
MBE	0.02	0.01	0.01	-0.26	-0.05	-0.07
R^2 *(%)*	99.96	99.67	98.84	99.75	99.11	98.12

TABLE 7. Assessment of estimated WS at heights 110-120m based on measurements at 10-100M.

Method	Deep neural network		Local wind shear exponent	
Height (m)	110	120	110	120
MAPE	0.79	1.37	1.53	2.92
RMSE	0.01	0.03	0.02	0.07
MBE	0.01	-0.03	-0.03	-0.04
R^2 *(%)*	99.92	99.76	99.80	99.18

as presented in Table 6. Moreover, the table shows that the proposed method outperformed the LWSE method.

In the seventh scenario, measured WSs between 10-100m, were used to estimate WS values at 110-120m. The error values, summarized in Table 7, were lower in magnitude than those in the previous cases. This is due to using more and more measured values of WS at lower heights for the estimation at higher heights.

IV. RESULTS ANALYSIS

In this section we analyze the results presented in the previous section and compare the performance of DNN with GANN. Table 8 summarizes the overall performance measures of DNN with LWSE at hub height (120m) based on measured values at lower heights. For example, the first column shows the performance indicators at 120m height based on measured WSs at 10-40m using the DNN and the LWSE methods. Similarly, the second column shows the results at 120m height based on measured WS values at 10-50m, and so on for the remaining columns. The table shows that the MAPE value is decreased from 11.66% to 9.65%, i.e. a reduction of about 17%, while estimating the WS by using measurements up to 50m instead of up to 40m. Almost similar magnitude of improvements was observed in the cases of RMSE and MBE values. The R^2 value also improved to 90.28% from 84.73%. The rate of decrease in error values slowed down as the number of measurement levels was increased. Therefore, this study concluded that measurements up to 50m are needed

TABLE 8. Comparison of Performance measures between DNN and LWSE methods at 120m.

	Measurements used at heights for the estimation of WSs															
Heights(m)	10-40		10-50		10-60		10-70		10-80		10-90		10-100		10-110	
Methods	DNN	LWSE	DNN	LWSE	DNN	LWSE	DNN	LWSE	DNN	LWSE	DNN	LWSE	DNN	LWSE	DNN	LWSE
MAPE	11.66	15.99	9.65	12.77	7.07	10.66	5.69	8.24	3.69	6.37	2.89	4.49	1.37	2.92	0.63	1.38
RMSE	1.25	1.92	0.97	1.24	0.45	0.88	0.3	0.54	0.15	0.33	0.11	0.17	0.03	0.07	0.01	0.02
MBE	0.38	-0.49	0.13	-0.32	-0.11	-0.27	-0.1	-0.17	-0.1	-0.12	0.01	-0.07	-0.03	-0.04	0	-0.01
R^2 (%)	84.73	81.80	90.28	87.44	95.19	90.75	96.8	94.19	98.45	96.36	98.84	98.12	99.76	99.18	99.96	99.83

TABLE 9. Comparison of Performance measures between DNN and GANN methods at 120m.

	Measurements used at heights for the estimation of WSs															
Heights (m)	**10-40**		**10-50**		**10-60**		**10-70**		**10-80**		**10-90**		**10-100**		**10-110**	
Methods	**DNN**	**GANN**	**DNN**	**GANN**	**DNN**	**GANN**	**DNN**	**GANN**	**DNN**	**GANN**	**DNN**	**GANN**	**DNN**	**GANN**	**DNN**	**GANN**
MAPE	11.66	21.56	9.65	9.79	7.07	8.58	5.69	6.61	3.69	3.72	2.89	3.63	1.37	1.47	0.63	0.88
RMSE	1.25	1.91	0.97	0.84	0.45	0.65	0.3	0.43	0.15	0.15	0.11	0.14	0.03	0.02	0.01	0.01
MBE	0.38	-0.05	0.13	0.14	-0.11	0.10	-0.1	0.22	-0.1	-0.10	0.01	0.11	-0.03	-0.04	0	0.04
R2 (%)	84.73	79.38	90.28	89.06	95.19	94.20	96.8	94.64	98.45	98.42	98.84	98.40	99.76	99.69	99.96	99.94

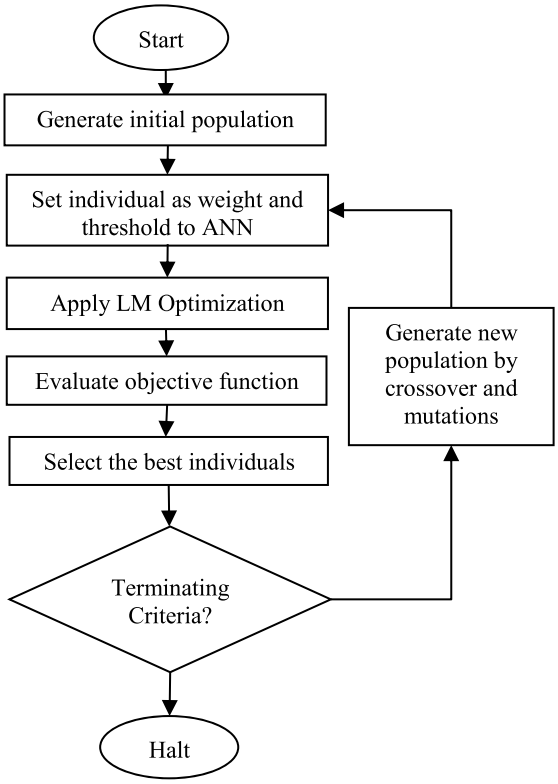

FIGURE 5. Training of GANN.

to achieve reasonable accuracies (MAPE less than 10% and R^2 more than 90%).

To further analyze the performance of the DNN as compared with other machine learning methods, we compare its performance with that of a hybrid system (GANN) that uses Genetic Algorithm (GA) to find a suitable initial weights and biases values for ANN. The GA is used along with the Levenberg-Marquart (LM) method to enhance the search capability for optimum weights and bias values [26], [35]. The combination of the GA and ANN is illustrated in Fig. 5. The LM algorithm is an iterative approach combining gradient descent and Gauss-Newton methods to minimize a function [36]. Parameters change their values at every iteration according to the following equation

$$W^{k+1} = W^{k} - \left[J^{T}J + \lambda I\right]^{-1} J^{T}(y - \bar{y}) \tag{10}$$

where W^{k+1} and W^{k} are the values of the weights at $(k+1)^{th}$ and k^{th} iterations, correspondingly. The Jacobian matrix J contains first derivatives of model output with respect to the optimizing parameters. Actual and predicted output values are denoted by y and $\bar{y}$, respectively. Increasing the damping parameter λ decreases the step size, and vice versa. Therefore, if a step is unacceptable, λ should be increased for a smaller step. If a step is accepted, λ is decreased in order to proceed more quickly in the correct descent direction, speeding up the convergence.

Ten initial populations were considered in the GA where each population represents a set of weights and bias values for ANN. Several trials and errors were used to select the algorithm parameters as follows: the number of hidden neurons equals twice the number of inputs organized in a single hidden layer, a maximum number of 150 iterations, initial weights and threshold values ranging between -30 to 30, a crossover rate of 0.8, and a mutation parameter of 0.01.

Similar to Table 8, the overall performance measures of DNN with GANN at hub height (120m) based on measured values at lower heights is shown in Table 9. The table shows that the performance of DNN is better than the performance of GANN in all measures.

The trends of the performance measures MAPE and R^2 are displayed in Fig. 6. Depending on the accuracy requirement for the resource assessment, the number of measurement levels can be chosen. For example, if an error of around MAPE=4% is tolerable, then measurements should be made up to 80m (Fig. 6(a)) and then extrapolated comfortably to the required hub height of 120m. Similarly, if R^2 of around 95%

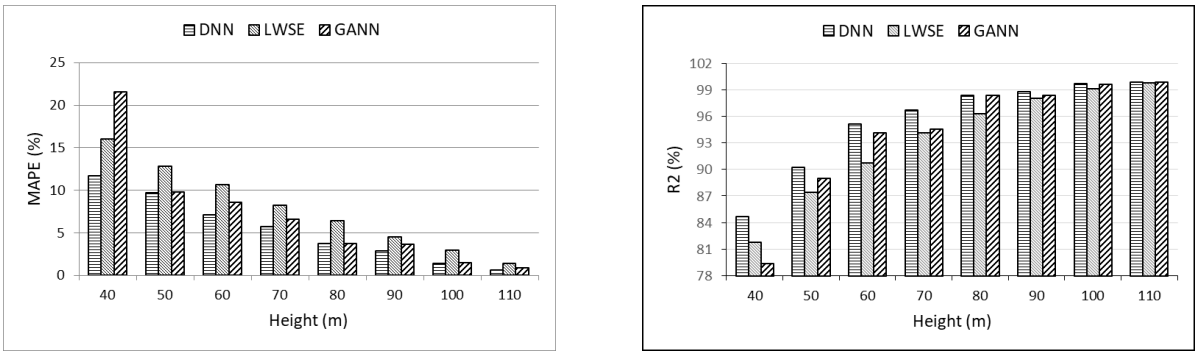

(a) (b)

FIGURE 6. (a). Trends of MAPE with measurement heights and (b). Trends of R^2 with measurement heights.

is required, then measurements should be made up to 60m as shown in Fig. 6 (b).

V. CONCLUSION

Commonly, the hub heights of modern wind turbines may be up to 120m. Hence, to carry out wind resource assessment correctly at the hub height, wind speed has to be measured or extrapolated to that height with minimum possible error. However, to address financial and technical constraints, wind speed measurements are commonly made at much lower heights. This is due to the fact that the cost of wind measurement masts increases tremendously with heights. This paper extrapolates WS at hub height using measured values at lower heights. The system was trained to find the WS at the next higher level. This extrapolated data was used along with the measured WS at lower heights to find WS at another higher level. This process was continued until the WS at 120m was estimated. These estimated WS values were compared with LiDAR system measured values using MAPE, RMSE, MBE, and R^2 as performance measures. This study concluded also that measurements up to 50m height are needed for acceptable accuracy of WS estimation at the hub height. Simulations indicate the superiority of the deep neural network when compared with local wind shear exponent method or with the standard feedforward neural network.

ACKNOWLEDGMENT

The authors would like to thank Saifur Rahman and MD. Saiful Islam for valuable discussions.

REFERENCES

[1] M. Sagrillo, "Incremental tower costs versus incremental energy," *Windletter*, vol. 25, no. 1, pp. 1–3, Jan. 2006.

[2] S. Kropper. (2011). *Wind Measurement Towers: How High Should They Be?* Accessed: Mar. 10, 2017. [Online]. Available: http://www.renewableenergyworld.com/articles/2011/01/wind-measurement-towers-how-high-should-they-be.html

[3] J. A. Businger, J. C. Wyngaard, Y. Izumi, and E. F. Bradley, "Flux-profile relationships in the atmospheric surface layer," *J. Atmos. Sci.*, vol. 28, no. 2, pp. 181–189, 1971.

[4] D. M. Carl, T. C. Tarbell, and H. A. Panofsky, "Profiles of wind and temperature from towers over homogeneous terrain," *J. Atmos. Sci.*, vol. 30, pp. 788–794, Jul. 1973.

[5] H. Tennekes, "The logarithmic wind profile," *J. Atmos. Sci.*, vol. 30, no. 2, pp. 234–238, 1973.

[6] U. Högström, "Non-dimensional wind and temperature profiles in the atmospheric surface layer: A re-evaluation," *Boundary-Layer Meteorol.*, vol. 42, pp. 55–78, Jan. 1988.

[7] S.-E. Gryning, E. Batchvarova, B. Brümmer, H. Jørgensen, and S. Larsen, "On the extension of the wind profile over homogeneous terrain beyond the surface boundary layer," *Boundary-Layer Meteorol.*, vol. 124, pp. 251–268, Aug. 2007.

[8] H. A. Panofsky, "Tower micrometeorology," in *Proc. Workshop Micrometeorol. Amer. Meteorol. Soc.*, D. A. Haugeb, Ed. 1973, pp. 151–176.

[9] U. Högström, A. S. Smedman, and H. Bergström, "Calculation of wind speed variation with height over the sea," *Wind Eng.*, vol. 30, no. 4, pp. 269–286, 2006.

[10] B. Lange, S. Larsen, J. Højstrup, and R. Barthelmie, "Importance of thermal effects and sea surface roughness for offshore wind resource assessment," *J. Wind Eng. Ind. Aerodyn.*, vol. 92, pp. 959–988, Sep. 2004.

[11] A. Peña and S. E. Gryning, "Charnock's roughness length model and non-dimensional wind profiles over the sea," *Boundary-Layer Meteorol.*, vol. 128, pp. 191–203, Aug. 2008.

[12] G. Gualtieri, "Surface turbulence intensity as a predictor of extrapolated wind resource to the turbine hub height: Method's test at an offshore site," *Renew. Energy*, vol. 111, no. 10, pp. 175–186, 2017.

[13] G. Gualtieri and S. Secci, "Comparing methods to calculate atmospheric stability-dependent wind speed profiles: A case study on coastal location," *Renew. Energy*, vol. 36, no. 8, pp. 2189–2204, 2011.

[14] J. F. Newman and P. M. Klein, "The impacts of atmospheric stability on the accuracy of wind speed extrapolation methods," *Resources*, vol. 3, no. 1, pp. 81–105, 2014.

[15] T. R. Ayodele, A. A. Jimoh, J. L. Munda, and J. T. Agee, "A statistical analysis of wind distribution and wind power potential in the coastal region of South Africa," *Int. J. Green Energy*, vol. 10, no. 8, pp. 814–834, 2013.

[16] A. Tizpar, M. Satkin, M. B. Roshan, and Y. Armoudli, "Wind resource assessment and wind power potential of Mil-E Nader region in Sistan and Baluchestan Province, Iran—Part 1: Annual energy estimation," *Energy Convers. Manage.*, vol. 79, pp. 273–280, Mar. 2014.

[17] D. Solyali, M. Altunç, S. Tolun, and Z. Aslan, "Wind resource assessment of Northern Cyprus," *Renew. Sustain. Energy Rev.*, vol. 55, pp. 180–187, Mar. 2016.

[18] D. Petković, Z. Ćojbašič, and V. Nikolić, "Adaptive neuro-fuzzy approach for wind turbine power coefficient estimation," *Renew. Sustain. Energy Rev.*, vol. 28, pp. 191–195, Dec. 2013.

[19] M. A. Mohandes, S. Rehman, and T. O. Halawani, "A neural networks approach for wind speed prediction," *Renew. Energy*, vol. 13, no. 3, pp. 345–354, 1998.

[20] D. Petković *et al.*, "Adaptive neuro-fuzzy maximal power extraction of wind turbine with continuously variable transmission," *Energy*, vol. 64, pp. 868–874, Jan. 2014.

[21] M. Mohandes, T. O. Halawani, S. Rehman, and A. A. Hussain, "Support vector machines for wind speed prediction," *Renew. Energy*, vol. 29, no. 6, pp. 939–947, 2004.

[22] V. Nikolić, S. Sajjadi, D. Petković, S. Shamshirband, Z. Ćojbašić, and L. Y. Por, "Design and state of art of innovative wind turbine systems," *Renew. Sustain. Energy Rev.*, vol. 61, pp. 258–265, Aug. 2016.
[23] D. Petković, N. T. Pavlović, and Z. Ćojbašić, "Wind farm efficiency by adaptive neuro-fuzzy strategy," *Elect. Power Energy Syst.*, vol. 81, pp. 215–221, Oct. 2016.
[24] M. Mohandes, S. Rehman, and S. M. Rahman, "Estimation of wind speed profile using adaptive neuro-fuzzy inference system (ANFIS)," *Appl. Energy*, vol. 88, no. 11, pp. 4024–4032, 2011.
[25] Y. S. Türkan, H. Y. Aydogmus, and H. Erdal, "The prediction of the wind speed at different heights by machine learning methods," *Int. J. Optim. Control, Theories Appl.*, vol. 6, no. 2, pp. 179–187, 2016.
[26] M. S. Islam, M. Mohandes, and S. Rehman, "Vertical extrapolation of wind speed using artificial neural network hybrid system," *Neural Comput. Appl.*, vol. 28, no. 8, pp. 2351–2361, 2017.
[27] Z. R. Shu, Q. S. Li, Y. C. He, and P. W. Chan, "Observations of offshore wind characteristics by Doppler-LiDAR for wind energy applications," *Appl. Energy*, vol. 169, pp. 150–163, May 2016.
[28] J. S. Rodrigo, F. B. Guillén, P. G. Arranz, M. S. Courtney, R. Wagner, and E. Dupont, "Multi-site testing and evaluation of remote sensing instruments for wind energy applications," *Renew. Energy*, vol. 53, pp. 200–210, May 2013.
[29] V.-M. Kumer, J. Reuder, and B. R. Furevik, "A comparison of LiDAR and radiosonde wind measurements," *Energy Procedia*, vol. 53, pp. 214–220, Jan. 2014.
[30] C. B. Hasager *et al.*, "Remote sensing observation used in offshore wind energy," *IEEE J. Sel. Topics Appl. Earth Observ. Remote Sens.*, vol. 1, no. 1, pp. 67–79, Mar. 2008.
[31] G. Hinton *et al.*, "Deep neural networks for acoustic modeling in speech recognition: The shared views of four research groups," *IEEE Signal Process. Mag.*, vol. 29, no. 6, pp. 82–97, Nov. 2012.
[32] G. E. Hinton and R. R. Salakhutdinov, "Reducing the dimensionality of data with neural networks," *Science*, vol. 313, no. 5786, pp. 504–507, 2006.
[33] S. Rehman, "Empirical model development and comparison with existing correlations," *Appl. Energy*, vol. 64, nos. 1–4, pp. 369–378, 2009.
[34] T. Reza, "Comparison result of inversion of gravity data of a fault by particle swarm optimization and levenberg-marquardt methods," *Springer Plus*, vol. 2, p. 462, Sep. 2013 doi: 10.1186/2193-1801-2-462.2013.
[35] C. D. Rosin, R. S. Halliday, W. E. Hart, and R. K. Belew, "A comparison of global and local search methods in drug docking," in *Proc. ICGA*, 1997, pp. 221–229.
[36] D. W. Marquardt, "An algorithm for least-squares estimation of nonlinear parameters," *J. Soc. Ind. Appl. Math.*, vol. 11, no. 2, pp. 431–441, 1963.

Authors' photographs and biographies not available at the time of publication.